Appl. Phys. A
DOI 10.1007/s00339-014-8270-1

Applied Physics A
Materials Science & Processing

INVITED PAPER

Near-field-enhanced, off-resonant laser sintering of semiconductor particles for additive manufacturing of dispersed Au–ZnO-micro/nano hybrid structures

Marcus Lau · Ralf G. Niemann · Mathias Bartsch · William O'Neill · Stephan Barcikowski

Received: 17 January 2014 / Accepted: 17 January 2014

Abstract Off-resonant near-field enhancement by gold nanoparticles adsorbed on crystalline zinc oxide significantly increases the energy efficiency of infrared laser sintering. In detail, ten different gold mass loads on zinc oxide were exposed to 1,064 nm cw-laser radiation. Variation of scan speed, laser power, and spot size showed that the energy threshold required for sintering decreases and sintering process window widens compared to laser sintering of pure zinc oxide powder. Transmission electron microscope analysis after focused ion beam cross sectioning of the sintered particles reveals that supported gold nanoparticles homogenously resolidify in the sintered semiconductor matrix. The enhanced sintering process with ligand-free gold nanoparticles gives access to metal–semiconductor hybrid materials with potential application in light harvesting or energy conversion.

Electronic supplementary material The online version of this article (doi:10.1007/s00339-014-8270-1) contains supplementary material, which is available to authorized users.

M. Lau · R. G. Niemann · S. Barcikowski (✉)
Technical Chemistry I, Center for Nanointegration Duisburg-Essen (CENIDE), University of Duisburg-Essen, Universitaetsstr. 7, 45141 Essen, Germany
e-mail: stephan.barcikowski@uni-due.de

M. Bartsch
Experimentalphysik, Center for Nanointegration Duisburg-Essen (CENIDE), University of Duisburg-Essen, Lotharstrasse 1, 47057 Duisburg, Germany

W. O'Neill
Institute for Manufacturing, University of Cambridge, 17 Charles Babbage Road, Cambridge CB3 0FS, UK

1 Introduction

Additive manufacturing by selective laser sintering produces 2D and 3D geometries with unique structures made of metals, insulators, or ceramics [1–4].

Nevertheless, if the process is applied for infrared (IR) laser-transparent materials like [5, 6] semiconductors, manufacturing of parts usually is inefficient due to low incoupling of laser energy. To relieve inefficiency either the laser wavelength can be changed toward the band gap energy of semiconductors, or the material response to the IR wavelength can be enhanced. The former is to be understood as resonant and the second off-resonant laser incoupling for sintering. Resonant laser sintering has been shown by Crespo-Monteiro et al. [7] who examined the influence of plasmonic silver nanoparticles (NP) on the laser intensity required to cause sintering. They showed that silver nanoparticles added to a mesoporous TiO_2 film enabled sintering at lower intensities with 488 nm laser light, hence exciting resonant surface plasmons of the added nanoparticles close to their plasmon band after adsorption (485 nm) [7]. Alternatively, also off-resonant excitation of gold particles by infrared laser radiation has been reported, making use of the near-field enhancement around the NP [8]. Hence, this method relies on the scattered near-field instead of energy absorption in the particle itself, in particular for ultra-short-pulsed lasers. For laser sintering cw lasers are widely applied, so that off-resonant near-field amplification could be a strategy to incouple energy into otherwise laser-transparent materials by supporting gold nanoparticles.

For this the amount of plasmonic particles should play an important role in the sintering process. For the investigation of off-resonant laser sintering process window we changed material response to laser irradiation by varying

Published online: 05 February 2014

the amount of surface-adsorbed gold nanoparticles on zinc oxide microparticles. Resonant laser sintering operates with shorter laser wavelength bearing the risk to approach ablation regimes by interband absorption, while off-resonant laser sintering adapts material parameters to IR laser light.

Pure zinc oxide is of interest as semiconductor with a direct band gap around 3.3 eV at 300 K and large exciton binding energy (60 meV) [9]. Further it is a cheap and an easy accessible material compared to rare earths, and recent efforts focus on, e.g. aluminum doped zinc oxide as transparent conductive thin films to substitute expensive indium tin oxide ITO [10].

Gold nanoparticles adsorbed on metal oxides are widely used in heterogeneous catalysis [11, 12] and ZnO-supported gold nanoparticles (ZnO@Au) were reported to enhance conversion efficiency of dye-sensitized solar cells [13] and to improve photocatalytic activity for high performance lithium ion batteries [14].

We present a strategy to enhance infrared laser sintering by gold nanoparticles (Au-NP) adsorbed on zinc oxide micro particles (ZnO-MP). For this purpose, ligand-free colloidal Au-NP generated by pulsed laser ablation in liquids (PLAL) are adequate candidates as they absorb with almost 100 % efficiency on micro particle surfaces [15, 16]. PLAL technique was first reported by Henglein and Fojtik [17] and since then drawn a steadily grown interest, as Au-NP in pure water show a remarkable high electrostatic stability without any surfactants [18, 19]. Here we combine the techniques of PLAL and laser sintering to enhance sintering processes and at the same time fabricating a nano/micro metal/semiconductor hybrid material.

Fig. 2 Top: calculated energy per section resulting from the applied power and writing velocities Bottom: process window and microscope pictures exemplarily shown for 0 and 5 wt % of gold nanoparticle loading on zinc oxide (see Supporting Information Fig. S2 for all process window diagrams). The sintering process window (*marked green*) has been quantified for all different gold loadings and plotted in Fig. 3 ▶

2 Experimental

2.1 Preparation of gold nanoparticles and adsorption on zinc oxide microparticles

Gold nanoparticles were produced by PLAL with a picosecond-pulsed Nd:YAG laser (1,064 nm) at 130 µJ pulse energy and 100 kHz focused on a gold target (99.00 % purity, Goodfellow) placed in an ablation chamber designed for PLAL filled with 100 ml deionized water [20, 21]. The concentration of obtained gold colloid was determined by differential weighting of the gold

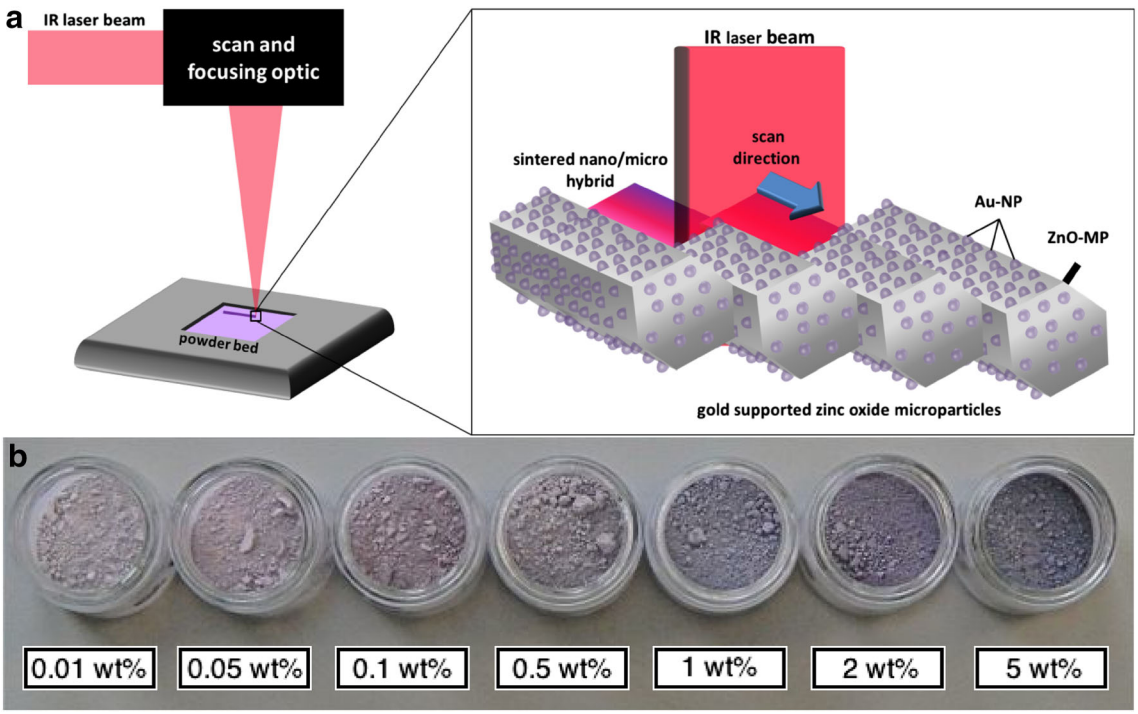

Fig. 1 **a** Illustration of laser sintering process and enhancement via gold nanoparticles supported on zinc oxide micro particles. **b** Zinc oxide micro particle powder with the increasing weight percentage of gold nanoparticles adsorbed on the particle surface

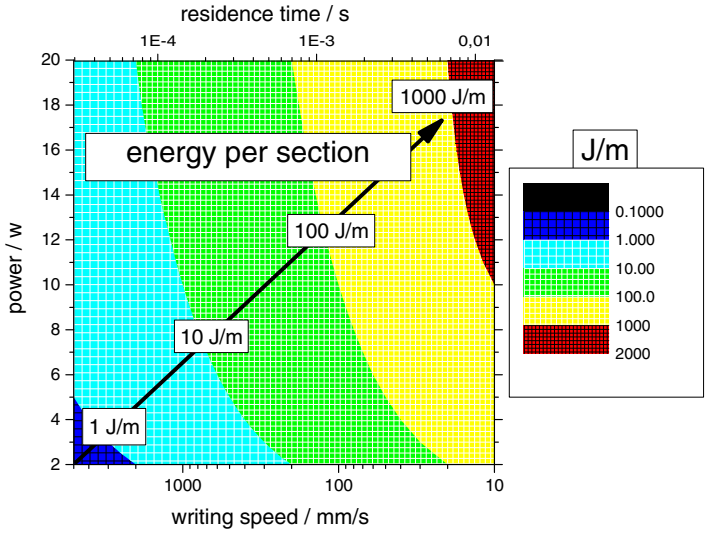
residence time / s
1E-4
1E-3
0,01
1000 J/m
energy per section
100 J/m
10 J/m
1 J/m
power / w
writing speed / mm/s
J/m
0.1000
1.000
10.00
100.0
1000
2000

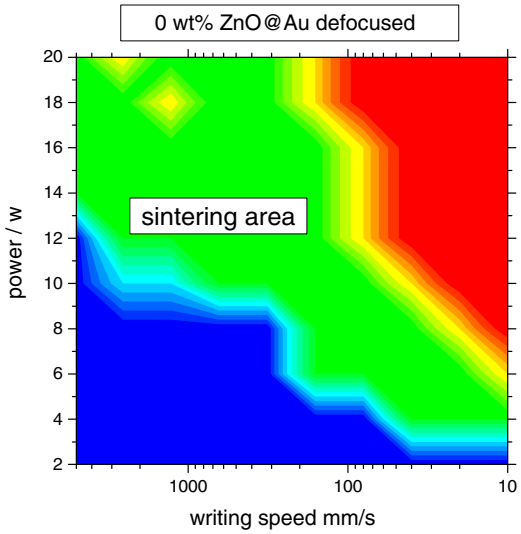
0 wt% ZnO@Au defocused
sintering area
power / w
writing speed mm/s

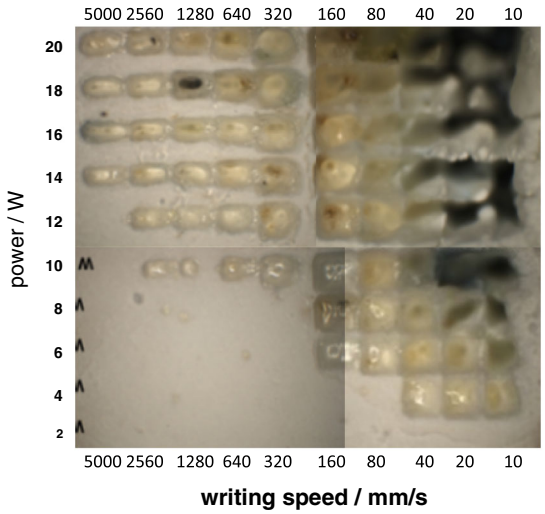
5000 2560 1280 640 320 160 80 40 20 10
power / W
writing speed / mm/s

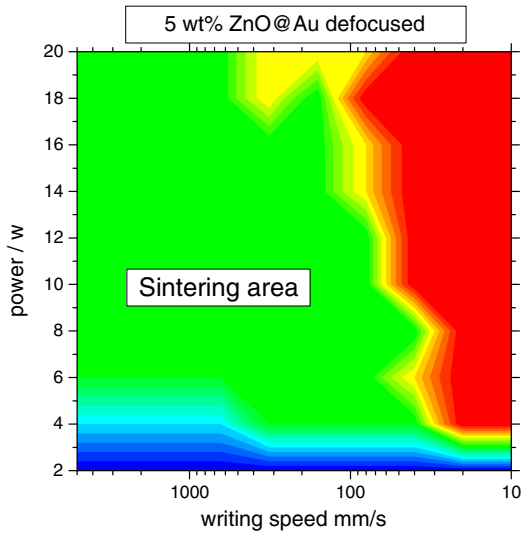
5 wt% ZnO@Au defocused
Sintering area
power / w
writing speed mm/s

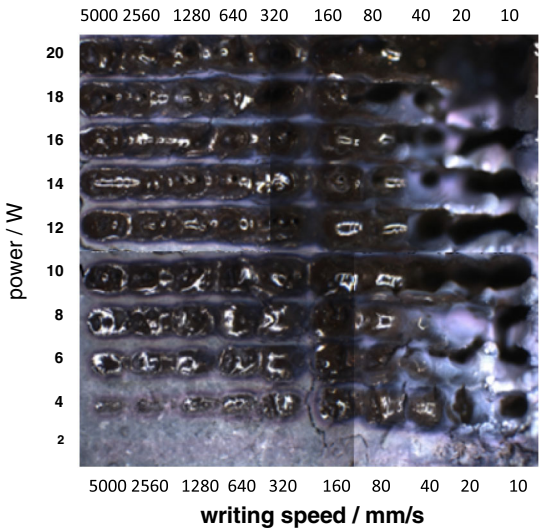
5000 2560 1280 640 320 160 80 40 20 10
power / W
writing speed / mm/s

target on a micro balance. After preparation of the Au-NP different amounts of ZnO-MP were suspended in the aqueous gold colloid to achieve corresponding loadings from 0.001 to 0.5 wt % gold on ZnO. The colloidal Au-NP adsorbed completely and homogenously onto the microparticle support within several hours. By subsequent sedimentation of the microparticles the transparent supernatant was decanted and particles were dried at 323 K for 12 h. After decompaction in a mortar ZnO-MP@Au-NP powders with weight ratios of 0, 0.001, 0.005, 0.01, 0.05, 0.1, 0.5, 1, 2, and 5 wt % shown in Fig. 1 were received.

2.2 Laser sintering of Au-NP supported ZnO-MP

To cover a broad spectrum of material response during laser sintering from no reaction to strong ablation and to obtain the sintering process in an appropriate manner, parameter studies of varying laser power and writing speed with two different spot sizes at the surface of powder bed were conducted. For this purpose, a powder bed of semiconductor micro particles has been prepared by manually compacting particles with a stamp, to obtain an even surface. Laser sintering has been performed with a fiber laser operating at 1,064 nm in cw-mode (G3, SPI Lasers PLC, redENERGY, SM-series). Applied laser power varied from 2 to 20 W in steps of 2 W. Writing speed of the laser has been varied from 10 to 5,000 mm/s. Each powder type with different gold load was treated with a 10 × 10 matrix with corresponding parameter pairs of power and writing speed. To have a detailed view of sintering behavior the laser beam was slightly focused to a spot size of 150 µm and for a stronger material response same parameters were applied with a spot size of 31 µm, resulting in higher intensities (up to 113.2 kW/cm^2 and 2.653 MW/cm^2, respectively). In the following the applied intensities will be considered as energy per section given in J/m, what takes the irradiation time into account.

Characterization of the irradiated powder bed surface was performed via imaging by an optical microscope. The material response to laser irradiation was evaluated from images shown in Supporting Information (Fig. S2) taken by the microscope. Each field of the 10 × 10 matrices from ten different gold loadings was evaluated and rated into the following five classes: no material response, transition from no response to sintering, sintering, and transition from sintering to ablation or ablation occurred (see Supporting Information Fig. S2). The total number of parameter pairs laser power and writing speed (for 150 µm spot diameter) resulting in successful sintering gives a quantitative value of the process window area. In the shown power-speed diagrams this area is marked green.

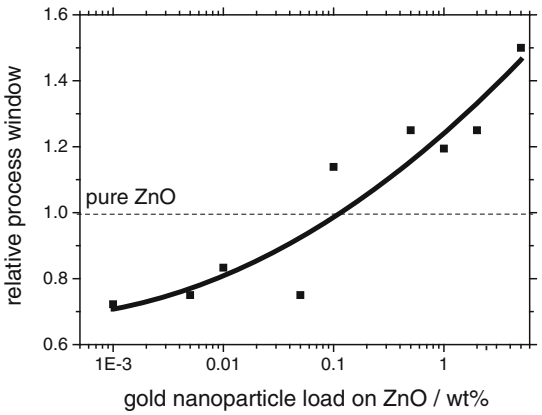

Fig. 3 Process window for laser sintering in dependence of gold nanoparticle load on zinc oxide microparticles (parameters of laser power, writing speed and laser spot size given in Supporting Information Fig. S2)

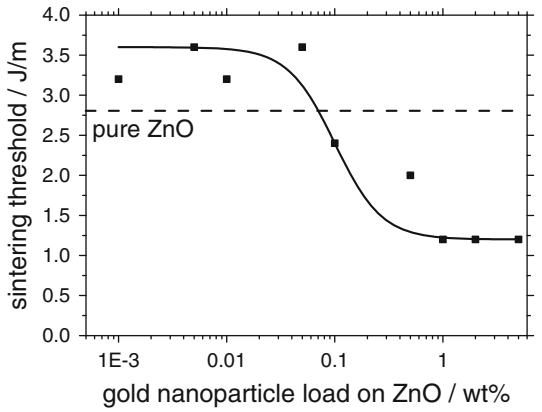

Fig. 4 Sintering threshold (minimum required energy per section) for writing speeds of 5 m/s for 150 µm spot size. Black dashed line shows threshold for pure zinc oxide microparticles without gold. Necessary energy per section first slightly increases for low gold nanoparticle loadings but than decreases significantly. Findings for sintering thresholds correlate with the widening of sintering process window, shown in Fig. 3

2.3 FIB cutting of supported micro particles and TEM analysis

A detailed insight into the gold-loaded micro particles, shown in Fig. 5, was enabled by cutting particles by a focused ion beam (FIB) and inspection of particle cross section in the transmission electron microscope (TEM) before and after sintering. SEM pictures taken during the FIB cutting process are shown in Fig. S1.

3 Results and discussion

The conducted experiments with varying power and writing speed show a curtail influence of gold nanoparticles to

material response on laser irradiation. At high gold loadings on zinc oxide microparticles the process window significantly extends compared to pure ZnO-MP. Pictures taken with the optical microscope and the corresponding power-speed diagrams are shown in Fig. 2 as well as the corresponding laser energy per section. The material response of pure ZnO-MP strongly differs compared to 5 wt % Au-NP loaded ZnO-MP regarding the threshold energy required for sintering. For 5 wt % gold nanoparticles on ZnO-MP sintering threshold decrease by a factor of 2.3 down to around 1 J/m. At this, it is impossible to define intensity thresholds or energy per section thresholds independently, as the former is not considering residence time of irradiation and the latter gives no information about focusing conditions. From diagrams shown in Fig. 2 and from Supporting Information it can be seen that higher intensities tend to lead to lower residence time to cause sintering, therefore reducing required energy per section.

Figure 3 shows the effect of gold nanoparticles on zinc oxide microparticles for the sintering process window. All values of the process window area are standardized to the value for pure zinc oxide. Low loadings of gold (0.001, 0.005, 0.01 and 0.05 wt %) result in narrower sintering process window, whereas loadings of 0.1 wt % significantly widen sintering process window up to 50 %.

Figure 4 depicts the sintering thresholds for different gold loadings obtained at 5 m/s with 150 µm spot size. The findings correlate with influence of gold nanoparticles to sintering process windows. For low gold loadings (up to 0.05 wt %), minimum required energy per section to cause sintering slightly increases from 2.8 J/m for pure zinc oxide microparticles to around 3.6 J/m. If the amount of gold nanoparticles is 0.1 wt % or higher, energy per section necessary to cause material response is reduced. Sintering threshold decreases down to 1.2 J/m for 1, 2 and 5 wt % of gold nanoparticles attached to microparticle support. Therefore, the highest reduction of sintering threshold by surface-adsorbed gold nanoparticles results in 57 % saved energy.

At low gold loads, reduction of process window and higher required energy per section for sintering can be explained by additional energy consumption for the melting of the added gold nanoparticles. At higher loadings, energy transfer to ZnO overcompensates, so that the sintering process window increases (and minimum required energy decreases) compared to pure ZnO. Surface-adsorbed Au-NP melt down and resolidify subsequently together with microparticles. This is verified by TEM pictures of FIB-sectioned microparticles in Fig. 5, showing zinc oxide microparticles with 5 wt % adsorbed Au-NP before and after sintering. Before laser sintering gold nanoparticles are homogenously distributed on the zinc oxide microparticles forming a rough surface. After laser treatment the gold nanoparticles are still visible in the TEM picture at the

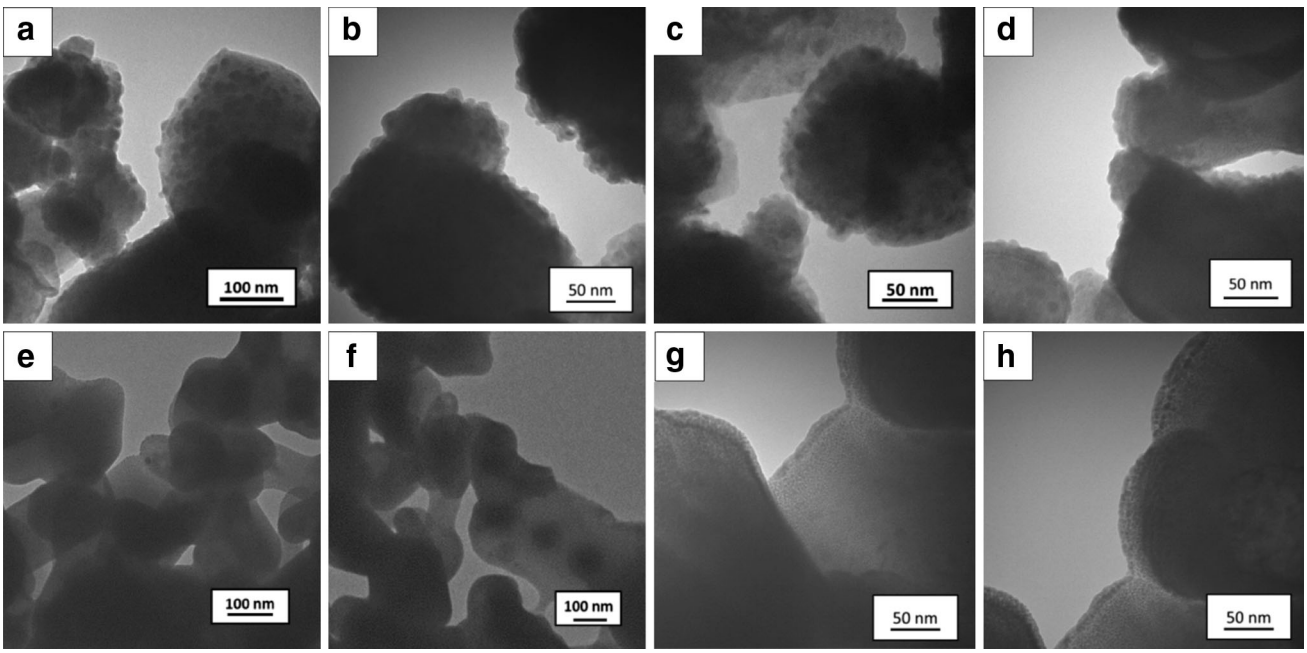

Fig. 5 TEM pictures taken from the ZnO microparticles with 5 wt % Au-NP loading prepared by the FIB method (see Supporting Information Fig. S1). Particles were cut by a focused ion beam and cross-sections subsequently analyzed in a TEM. Before laser sintering surface-adsorbed gold nanoparticles form a rough surface (**a**–**d**). TEM pictures taken after laser sintering of the supported micro and submicro particles reveal a sintering of the particles and a less rough surface after laser treatment (**e**–**h**)

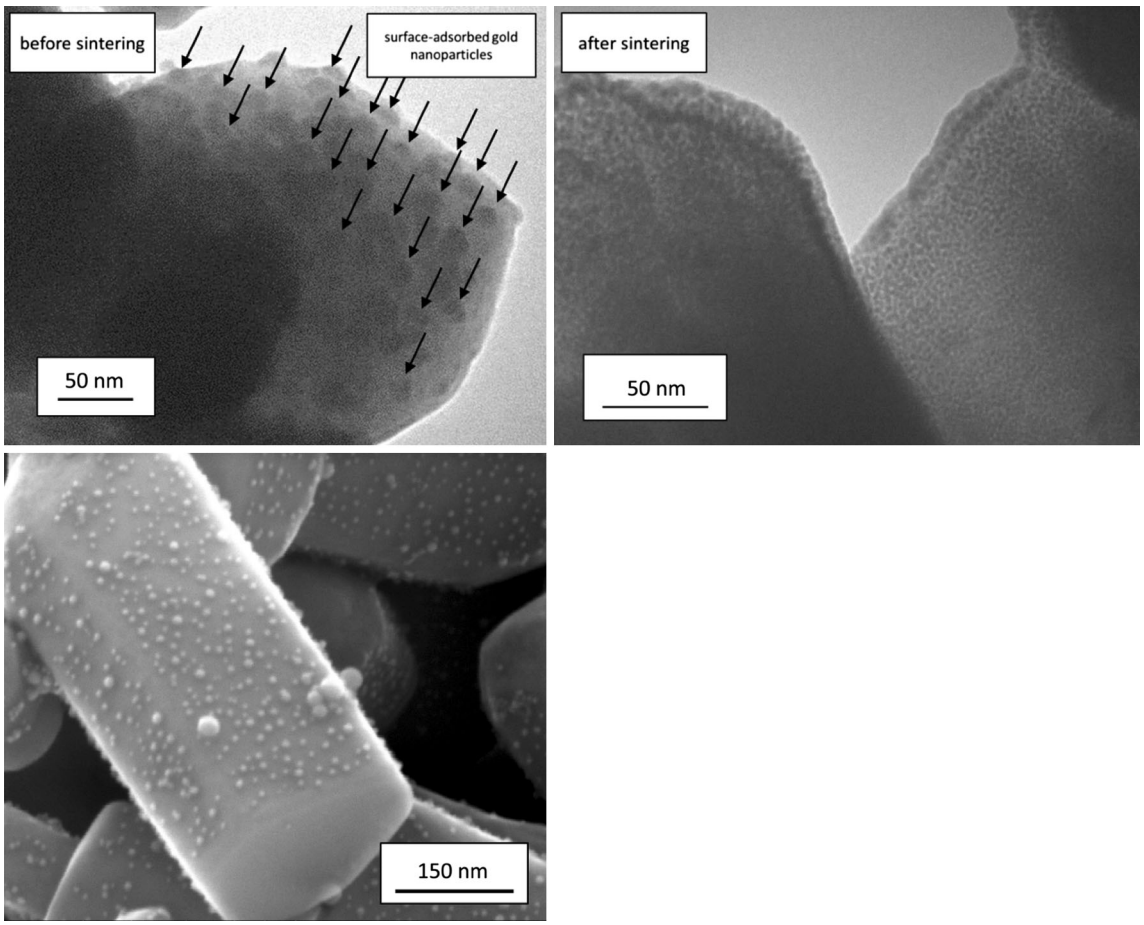

Fig. 6 TEM pictures showing the ultra-structure before (*left*) and after (*right*) laser sintering. SEM picture at the bottom demonstrates homogenous distribution of laser-generated gold nanoparticles supported on zinc oxide microparticles

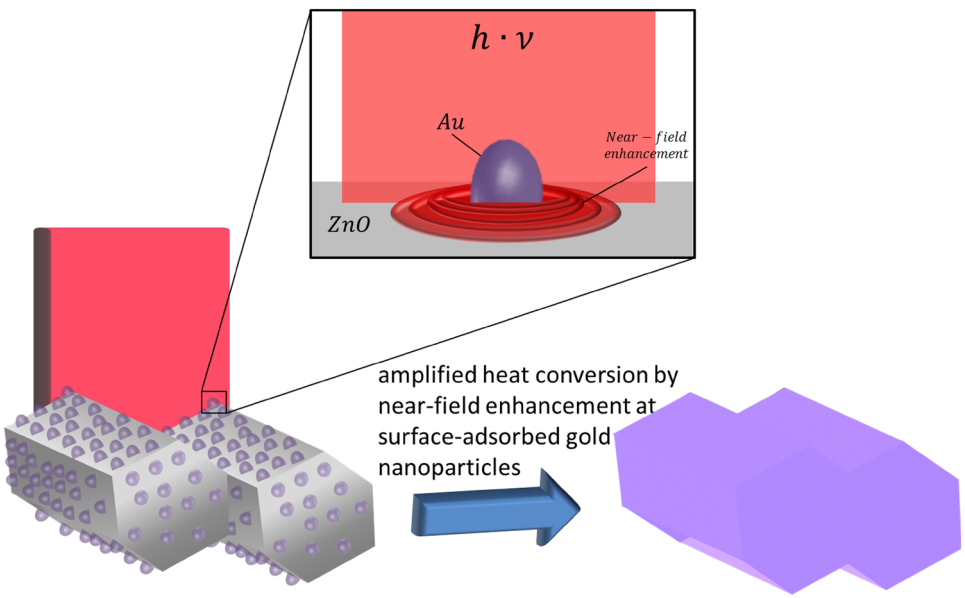

Fig. 7 Schematic illustration of the supposed mechanism and material response during off-resonant near-field enhancement of infrared laser sintering. Amplification of IR laser in vicinity of the gold particle leads to energy and heat transfer to infrared transparent zinc oxide, and subsequent melting of gold nanoparticles and zinc oxide, followed by resolidification forming smooth gold-semiconductor hybrid surface

cross section, but seem to be embedded under a smooth and homogenous ZnO microparticle surface. Thus, a hybrid gold-semiconductor structure has been achieved by additive manufacturing (Fig. 6).

Beside the enhancement of laser sintering efficiency, laser irradiation of surface-adsorbed gold nanoparticles might be a method for the fabrication of homogenous micro/nano semiconductor/metal compounds with a smooth and homogenous surface. This shows that PLAL-generated gold nanoparticles not only adsorb easily on metal oxide surfaces but also that the resulting nanostructured surface adsorbate can further be influenced and post-treated by laser irradiation.

Crespo-Monteiro et al. [7] showed that mesoporous TiO_2 films can be sintered at intensities of 97 kW/cm^2 with 244 nm cw-laser light. The ablation regime was determined to start at 242 kW/cm^2. Sintering of TiO_2 at 488 nm did not show any material response up to 3 MW/cm^2 but sintering threshold could be reduced to 0.4 kW/cm^2, if plasmonic silver nanoparticles were added to the TiO_2. Also non-plasmonic silver oxide enabled sintering at 488 nm, what indicates that off-resonant near-field enhancement by scattering may happen in this case as well. We examined the influence of gold to IR laser sintering whereby low amounts of Au-NP reduce laser process window. However, already 0.1 wt % of gold adsorbed on the semiconductor support results in an enhancement of process window area and decreasing thresholds for material response.

From Fig. 2 the ablation threshold can be determined to be around 100 J/m for loaded and unloaded zinc oxide for spot sizes of 150 µm. If the spot diameter is decreased to 31 µm ablation threshold decreases (Supporting Information Fig. S2). This leads to the assumption that for high laser intensities energy transfer from gold nanoparticles can even evaporate the molten states.

Due to the observations we propose an off-resonant near-field enhancement to cause effective material melt down of ZnO microparticle surface. In case of gold nanoparticle loadings below 0.1 wt % heat transfer to the carrier material is not sufficient to melt microparticle surface. For higher loadings, Au-NP transfer enough energy to the zinc oxide. This energy is converted locally into heat resulting in surface melting and resolidification leaving the sintered micro/nano hybrid structure. Figure 7 illustrates the assumed mechanism for efficiency increase of laser sintering, where near-field enhancement potentially plays a key role. However, it cannot be excluded that direct excitation and heating of the gold nanoparticles contribute to the heat transfer to ZnO as well. It is known that aggregation of plasmon resonant particles causes plasmon coupling leading to bathochromic shift. We expect this effect not to be dominant, since the visible absorption (color) of the gold-ZnO-material even at high loading rates does not indicate a strong SPR shift. Hence only a weak absorption is expected at the applied laser wavelength. In addition, it is known that particle aggregation increases their extinction coefficient mainly by (off-resonant) scattering.

4 Conclusions

Adsorption of gold nanoparticles, synthesized by laser ablation in liquids, can enhance laser sintering of semiconductors. If an adequate amount of gold nanoparticles is brought to the surface of the target material, significantly less (57 %) energy input is required to cause a material reaction. This is of particular interest for additive manufacturing whereby lower laser power for sintering is necessary or productivity may be increased. Further, laser irradiation of the adsorbate fabricates micro/nano ZnO/Au compounds with dispersed ultra-structure. The presented experimental data present a novel approach in additive manufacturing giving access to enhanced laser sintering and at the same time surface modification of semiconductors creating metal hybrid materials. Such materials may be of interest for energy application, where light has to be converted into current, or current into light, by combining the semiconductor bandgap with the electron capacity of the metal.

Acknowledgments The authors thank Jurij Jakobi for TEM measurements.

References

1. S. Hong, J. Yeo, G. Kim, D. Kim, H. Lee, J. Kwon, H. Lee, P. Lee, S. Ko, ACS Nano **7**, 5024 (2013)
2. M. Agarwala, D. Bourell, J. Beaman, H. Marcus, J. Barlow, Rapid Prototyp. J. **1**, 26 (1995)
3. N. Tolochko, Y. Khlopkov, S. Mozzharov, M. Ignatiev, T. Laoui, V. Titov, Rapid Prototyp. J. **6**, 155 (2000)
4. S. Dudziak, M. Gieseke, H. Haferkamp, S. Barcikowski, D. Kracht, Phys. Procedia **5**, 607 (2010)
5. B. Zhu, C. Xie, A. Wang, J. Wu, R. Wu, J. Liu, J. Mater. Sci. **42**, 5416 (2007)
6. Y. Kathuria, Surf. Coat. Technol. **116**, 643 (1999)
7. N. Crespo-Monteiro, N. Destouches, L. Saviot, S. Reynuad, T. Epicier, E. Gamet, L. Bios, A. Boukenter, J. Phys. Chem. C **116**, 26857 (2012)
8. É. Boulais, R. Lachaine, M. Meunier, Nano Lett. **12**, 4763 (2012)
9. Ü. Özgür, Y.I. Alivov, C. Liu, A. Teke, M.A. Reshchikov, S. Doğan, V. Avrutin, S.-J. Cho, H. Morkoç, J. Appl. Phys. **98**, 41301 (2005)
10. S.N. Bai, T.Y. Tseng, Thin Solid Films **515**, 872 (2006)
11. M. Haruta, Catal. Today **36**, 153 (1997)
12. S. Hashmi, G. Hutchings, Angew. Chem. Int. Ed. **45**, 7896 (2006)
13. V. Dhas, S. Muduli, W. Lee, S. Han, S. Ogale, Appl. Phys. Lett. **93**, 243108 (2008)

14. M. Ahmad, S. Yingying, A. Nisar, H. Sun, W. Shen, M. Weie, J. Zhu, J. Mater. Chem. **21**, 7723 (2011)
15. S. Barcikowski, G. Compagnini, Phys. Chem. Chem. Phys. **9**, 3022 (2013)
16. P. Wagener, A. Schwenke, S. Barcikowski, Langmuir **28**, 6132 (2012)
17. A. Fojtik, A. Henglein, Ber. Bunsenges. Phys. Chem. **97**, 252 (1993)
18. S. Barcikowski, F. Devesa, K. Moldenhauer, J. Nanoparticle Res. **11**, 1883 (2009)
19. C. Rehbock, V. Merk, L. Gamrad, R. Streubel, S. Barcikowski, Phys. Chem. Chem. Phys. **15**, 3057 (2013)
20. P. Nachev, D. Zand, V. Coger, P. Wagener, K. Reimers, P. Vogt, S. Barcikowski, A. Pich, J. Laser Appl. **24**, 1 (2012)
21. P. Wagener, A. Schwenke, B. Chichkov, S. Barcikowski, J. Phys. Chem. C **114**, 7618 (2010)